

Corotating interaction regions (CIRs) at sub-harmonic solar rotational periods and their impact on ionosphere-thermosphere system during the extreme low solar activity year 2008

S Tulasi Ram^{1,2,§,*}, M Yamamoto¹, B Veenadhari³, Sandeep Kumar³ & S Gurubaran²

¹Research Institute for Sustainable Humanosphere (RISH), Kyoto University, Uji, Japan

²Equatorial Geophysical Research Laboratory (EGRL), Indian Institute of Geomagnetism, Tirunelveli 627 011, India

³Indian Institute of Geomagnetism, New Panvel, Navi Mumbai 410 218, India

[§]E-mail: tulasi@iigs.iigm.res.in

Received October 2011; accepted 23 February 2012

The past solar minimum year 2008 has been exceptionally quiet with more than 70% spotless days and the solar EUV irradiance and F10.7 solar flux levels steadily at low values for a prolonged period. During this unique solar minimum epoch, however, the geospace environment is recurrently intercepted by solar wind high speed streams from the low-latitude coronal holes, which are the primary contributors for recurrent geomagnetic activity at solar rotational (27-day) and its sub-harmonic (13.5 and 9-day) periodicities. In response, both the neutral and ionized upper atmospheric properties continued to ring with same periodicities. The results indicate that both the neutral and electron density response at 400 km (topside ionosphere) is dominated by the changes in temperature and/or scale height and exhibits coherent enhancements concurrently with the periodicities in geomagnetic activity. However, the equatorial electrojet (EEJ) strength does not exhibit any recurrent signatures at these periodicities.

Keywords: Corotating interaction regions (CIRs), Equatorial electrojet (EEJ) strength, Solar rotational periodicity, Solar wind parameters, Geomagnetic activity indexes, Electron density, Neutral density

PACS Nos: 94.20.wg; 96.60.Ub

1 Introduction

The ionosphere-thermosphere system is susceptible to the forces originating both below from lower atmosphere as well as above from solar and magnetospheric driven sources. The past minimum epoch between solar cycles 23 and 24 has been exceptionally quiet with sunspot numbers at their lowest in the past 75 years, causing the ionosphere and thermosphere system in a steady, low solar flux preconditioned state for a prolonged period. Under these prevailing low solar activity conditions, one would expect to minimize the solar-driven and magnetospheric disturbances and provide opportunity to study the dynamics of ionosphere-thermosphere system driven by the forces coupled from the lower atmosphere. As such, several interesting findings have been reported such as DE3 non-migrating tides and 4-peak longitudinal structure of equatorial ionization anomaly (EIA)¹⁻⁴, semi-diurnal perturbations driven by sudden stratospheric warming events⁵⁻¹⁰, and planetary wave signatures at quasi 2-day and 16-day

periodicities¹¹⁻¹⁴. However, accompanying to this low solar activity epoch, there were also fast recurrent solar wind streams associated with large, long-lived low latitude coronal holes on Sun and the resultant recurrent geomagnetic disturbances that have significant impact on ionosphere-thermosphere system^{15,16}.

The coronal holes (CHs) and solar wind (SW) streams undergo systematic variations over the 11-year solar cycle. Through much of the cycle, the Sun's polar region is dominated by CHs, the sources of large, persistent and fast SW streams with an average bulk speed of 500 – 800 km s⁻¹ (Ref. 17). During the solar minimum, the polar holes became large and extend into equatorial and low-latitude regions emanating fast SW streams in equatorial plane that are more geo-effective^{18,19}. In addition to fast streams from CHs, the SW has dense low-speed streams (300 – 400 km s⁻¹) from the closed-field regions near the equator, known as equatorial coronal streamer belt. As the streams travel in the interplanetary space, the high-speed streams catch the

preceding low-speed streams and create regions of enhanced density and magnetic field, called corotating interaction regions (CIRs)²⁰. When the coronal high-speed wind stream interacts with the preceding slow wind stream, forward and reverse shocks often form around the CIR boundaries. The CIR interfaces can be characterized by a relatively sharp density drop, a temperature rise, and a sharp increase in the SW bulk velocity. Since the CHs have tendency to rigidly rotate with Sun and persist for several solar rotations, the CIR interfaces also repeat for several solar rotations inducing recurrent geomagnetic disturbances at ~27-day periodicity.

Both the neutral and ionized upper atmosphere undergoes significant modifications due to the changes in the thermosphere composition, neutral density, temperature, neutral winds as well as the electric fields, which in turn greatly varies with latitude, altitude, local time, season and the phase of the geomagnetic activity. Since various neutral and electrodynamic coupling processes are involved, the response of global thermosphere – ionosphere system to geomagnetic storms is much complex and been the subject of extensive investigations by both case studies as well as model simulations during the past 3–4 decades^{21–27}. However, the earlier studies on the topside ionospheric response to geomagnetic storms were mostly based on the case studies of isolated geomagnetic storms. Although the amplitude is smaller, the CIRs produce ionospheric changes similar to those associated with isolated geomagnetic storms²⁸. CIRs are especially prominent during the declining phase of the solar cycle, when the heliospheric magnetic field has a well-developed sector structure and CHs extend to low latitudes²⁹. Therefore, the past solar minimum epoch provides an excellent opportunity to study the characteristics of CIRs, recurrent geomagnetic activity and their impact on geospace environment. The year 2008 represents the extremely low solar activity period with more than 70% spotless days (the annual mean sunspot number is only three) and global weakness in the heliospheric magnetic field³⁰, hence, considered for this study.

2 Data

The interplanetary solar wind and magnetic field parameters measured by Atmospheric Composition Explorer (ACE) satellite at L1-point available through the National Space Science Data Center's OMNIWeb interface (<http://nssdc.gsfc.nasa.gov/omniweb/>) during the low solar activity year 2008 were considered in

this study. The geomagnetic activity data such as AE, Kp and SymH-indices are obtained from World Data Center for Geomagnetism, Kyoto University (<http://wdc.kugi.kyoto-u.ac.jp/>). The neutral density observations from the triaxial accelerometer onboard the CHALLENGING Mini-satellite Payload (CHAMP) satellite were examined to study the thermospheric response to recurrent geomagnetic activity. All the measurements during this period of study are normalized to this fixed altitude of 400 km to remove density variations due to height changes of satellite orbits (<http://sisko.colorado.edu/sutton/>). Further, the global vertical electron density observations of Formosat3/COSMIC (F3/C) radio occultation experiment were also considered to study the electron density response. F3/C is a constellation of six microsattellites orbiting at about 800 km altitude, 72° inclination angle, and 30° separation in longitude. Each F3/C satellite has a GPS Occultation eXperiment (GOX) payload, performing the radio occultation observations in the ionosphere and provides ~2000 vertical electron density profiles per day, which are uniformly distributed all over the globe^{3,4,16}. Finally, in order to examine the electric field perturbations, the equatorial electroJet (EEJ) strength data derived from two ground based magnetometers from Indian network of magnetometers, one at the equatorial station Tirunelveli (8.7°N geog latitude, 77.8°E geog longitude and 0.6°N dip latitude) and another at an off-equatorial station Alibagh (18.5°N geog latitude, 72.9°N geog longitude and 12.9°N dip latitude) have been considered.

3 Results

3.1 Corotating Interaction Regions (CIRs) during 2008

When the fast SW stream from CH takes over the preceding slow SW stream, an interaction region is formed in the vicinity of border between the two streams. A forward and reverse shock may also produce in the preceding slow stream and trailing fast stream, respectively. This structure of interaction corotates with the Sun, hence, giving rise to the name corotating interaction regions (CIRs). The classical features of CIRs are well described in literature^{20,31,32}. When CIR sweeps across the observing satellite (ACE), all the SW parameters such as magnetic field strength, velocity, temperature and the density exhibit an increase at the forward shock. At the stream interface, which is the boundary between the slow solar wind and fast stream, the temperature and

velocity increase sharply while the SW density exhibits a sharp decrease. Across the reverse shock, the SW density and magnetic field decreases while the velocity further increases or may remain at high levels. It may be noted that all the CIR interfaces may or may not accompany with the forward and reverse shocks. For example, Fig. 1 shows the three recurrent CIRs observed by ACE satellite during the year 2008. Figure 1(a-e) shows the variations of SW magnetic field strength (|B|), SW proton velocity (V_p), temperature (T_p), density (N_p) and z-component of interplanetary magnetic field (IMF B_z) in GSM coordinates, respectively for the period from day numbers 310 to 335 in 2008. The typical features of stream interface such as sharp rise in SW temperature (T_p) and velocity (V_p) accompanied with sudden drop in density (N_p) can be clearly observed as indicated with solid vertical lines in red color. The forward and reverse shocks are indicated in green dashed lines. Further, the IMF B_z exhibits fast positive and negative excursions at stream interfaces that would possibly lead to the development of geomagnetic storms of weak to moderate intensity.

Figure 2 from top to bottom shows the variations of F10.7 solar flux, solar EUV irradiance at 50-105 nm, interplanetary magnetic field magnitude (|B|), SW proton velocity (V_p), temperature (T_p), density (N_p),

z-component of interplanetary magnetic field (IMF B_z), AE index, Kp index and Sym-H index, respectively, as a function of day number during low solar activity year 2008. It can be seen from Fig. 2(a) that the 10.7 cm solar flux index (F10.7) remains steady at low values of ~ 70 solar flux units during the entire period of 2008 indicating a very low solar activity state. The solar EUV irradiance at 50 to 105 nm wavelengths varies between $2.4e-3$ to $2.8e-3$ W m⁻² [Fig. 2(b)]. The most striking feature seen from this figures is a series of sharp pluses in magnetic field strength (|B|) and solar wind density (N_p) [Figs 2(c) and (f)] and subsequent enhancements in solar wind velocity (V_p) and temperature (T_p) [Figs 2(d) and (e)]; the density pulses [Fig. 2(f)] are also sharpest due to its sudden decrease while the velocity and temperature [Figs 2(d) and (e)] continue to increase. As described, these are the typical features of CIRs, and a series of 38 recurrent CIRs are identified during this year 2008. Further, the IMF B_z exhibits fast positive and negative excursions around the stream-stream interface region which is the typical feature of Alfvén waves within the CIRs³³. The negative excursions of IMF B_z would possibly lead to magnetic reconnection which causes recurrent geomagnetic activity as can be observed from the variations of AE, Kp and SymH indices [Figs 2(h-k)].

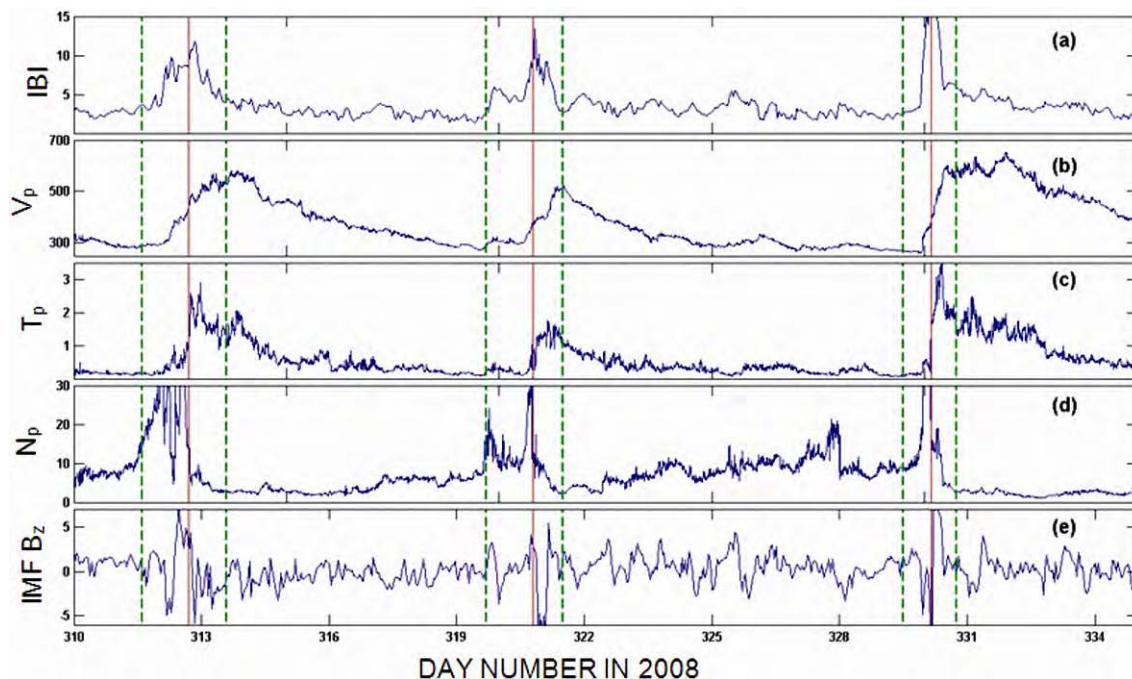


Fig. 1 — Recurrent corotating interaction regions (CIRs) in the interplanetary solar wind and magnetic properties; Panels from top to bottom show variations of: (a) solar wind magnetic field strength (|B|); (b) solar wind proton velocity (V_p); (c) temperature (T_p); (d) density (N_p); and (e) IMF B_z for the period from day numbers 310 to 335 in 2008

However, because of the oscillatory nature of IMF Bz, the resultant geomagnetic storms are typically of only weak to moderate intensity³⁴. From the variation of SymH-index [Fig. 2(k)], it can be clearly seen that there were a series of recurrent geomagnetic storms of moderate to less intensity (~ -60 to -40 nT) during this period.

3.2 Sub-harmonic solar rotational periodicities in SW and geomagnetic activity

With a view to examine the periodicities in the CIRs and recurrent geomagnetic activity, the Lomb-Scargle (LS) periodograms^{35,36} of various parameters shown in Fig. 2 are computed and presented in Fig. 3. The horizontal dashed lines in Fig. 3 indicate the 95% significant levels. The most striking features that can be observed from LS periodograms is that all the SW parameters (|B|, Vp, Tp and Np) as well as the geomagnetic activity indices (AE, Kp and SymH) during this period exhibit pronounced spectral peaks at solar rotational (27-day) and its sub-harmonic (13.5 and 9-day)

periodicities. Further, the spectral peak at 9-day periodicity is very sharp and strongest in the SW and geomagnetic parameters. In contrast, the F10.7 solar flux and EUV irradiance, though exhibit 27-day periodicity; do not exhibit any significant spectral peaks at 13.5 and 9-days. Therefore, the results from Figs 2 and 3 clearly suggest that these short-period sub-harmonic solar rotational periodicities at 13.5 and 9-day periods in geomagnetic activity indices (AE, Kp and SymH) are primarily due to SW energy input associated with high speed streams (HSS) from recurrent CHs.

3.3 Thermosphere-Ionosphere response

The investigation is focused to the response of thermosphere and ionosphere to this recurrent geomagnetic activity. Although the intensity is small, the geomagnetic storms induced by recurrent HSS-CIR structures may also significantly alter thermospheric and ionospheric densities²⁸. With a view to investigate this, the thermospheric neutral density observations from CHAMP satellite and

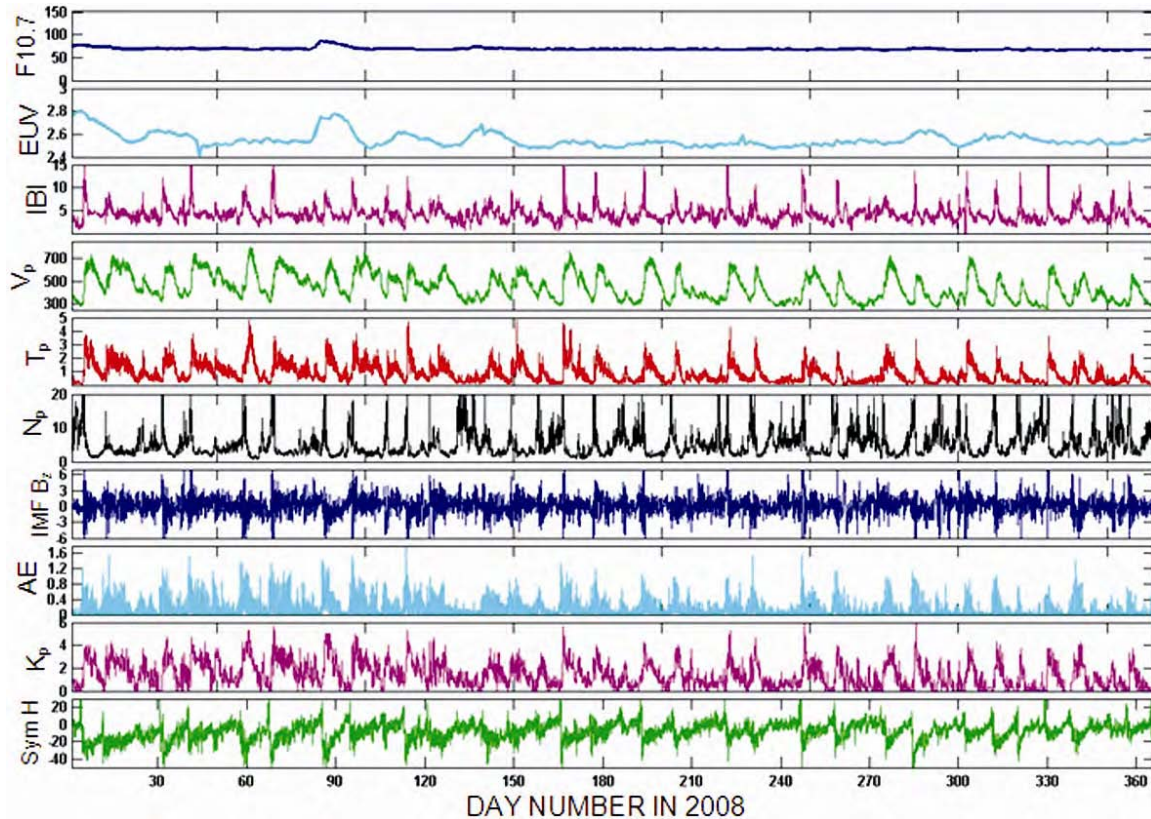


Fig. 2 — Recurrent geomagnetic storms associated with HSS-CIR structures in extreme low solar activity year 2008; Panels from top to bottom show variations of: (a) F10.7 solar flux; (b) solar EUV irradiance; (c) solar wind magnetic field strength (|B|); (d) proton bulk velocity (Vp); (e) temperature (Tp); (f) density (Np); (g) IMF Bz; (h) AE index (divided by 1000 for simplicity); (i) Kp index; and (j) SymH index as a function of day number in 2008

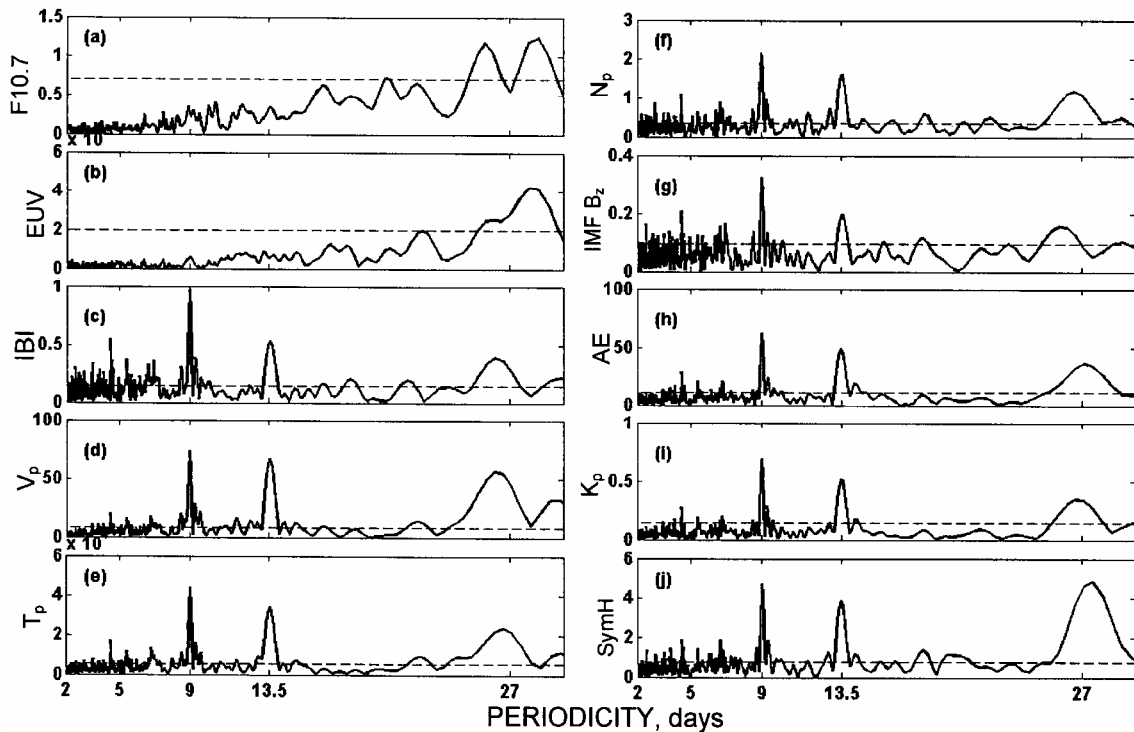


Fig. 3 — Lomb-Scargle (LS) periodograms of: (a) F10.7 solar flux; (b) solar EUV irradiance; (c) solar wind magnetic field strength (IBI); (d) proton bulk velocity (V_p); (e) temperature (T_p); (f) density (N_p); (g) IMF B_z ; (h) AE index; (i) K_p index; and (j) SymH index during the year 2008; horizontal dashed line indicates the 95% significant levels

electron density observations from COSMIC Radio Occultation experiment at the altitude of 400 km have been considered. Both the neutral density and electron density data observations have been binned into 31 latitudinal bins of 5° window from -75° to 75° geographic latitudes. The density observations at all the longitudes/local times in a day for each latitudinal bin are then averaged to compute daily zonal mean densities. Figure 4 shows the daily zonal mean neutral density from CHAMP [Fig. 4(a)] and electron density from F3/C [Fig. 4(b)] at 400 km altitude as a function of geographic latitude and day number in the year 2008. Superimposed black curve in Figs 4(a and b) is the variation of 3-hr K_p index during the year 2008 with scale on right hand side. It can be clearly seen from these figures that both the neutral density [Fig. 4(a)] as well as the electron density [Fig. 4(b)] at 400 km exhibits concurrent enhancements with K_p index throughout this period. In order to further examine the sub-harmonic solar rotational periodicities in thermosphere and ionosphere, the LS spectral analysis is performed on neutral and electron densities at each latitudinal bin and the periodograms are presented in Figs 5(a) and 5(b), respectively. The LS periodogram of the

geomagnetic activity index K_p is also superimposed (black curve with right hand side scale) in Figs 5(a and b). Predominant spectral amplitudes can be observed at solar rotational (27-day) and its sub-harmonic periods (13.5 and 9-days) in both neutral and electron densities globally at all latitudes. Further, the spectral amplitudes at these periodicities correspond extremely well with the periodicities in the geomagnetic activity index (K_p).

Further, with a view to examine the phase relationship between the perturbations in thermospheric and ionospheric densities with the recurrent geomagnetic activity, the quasi-periodic oscillations in zonal mean neutral and electron densities corresponding to 9-day periodicity for each latitude bin are spectrally filtered. A digital FIR band-pass filter centered at 9 days with half power points at 6 and 12 days is employed. Figures 5(c and d) show the band-pass filtered 9-day quasi periodic perturbations in neutral and electron densities at 400 km, respectively as a function of latitude and day number. The perturbations in both neutral density and electron density are expressed as the relative percentage with respect to background levels (81-day running average). The band-pass filtered 9-day

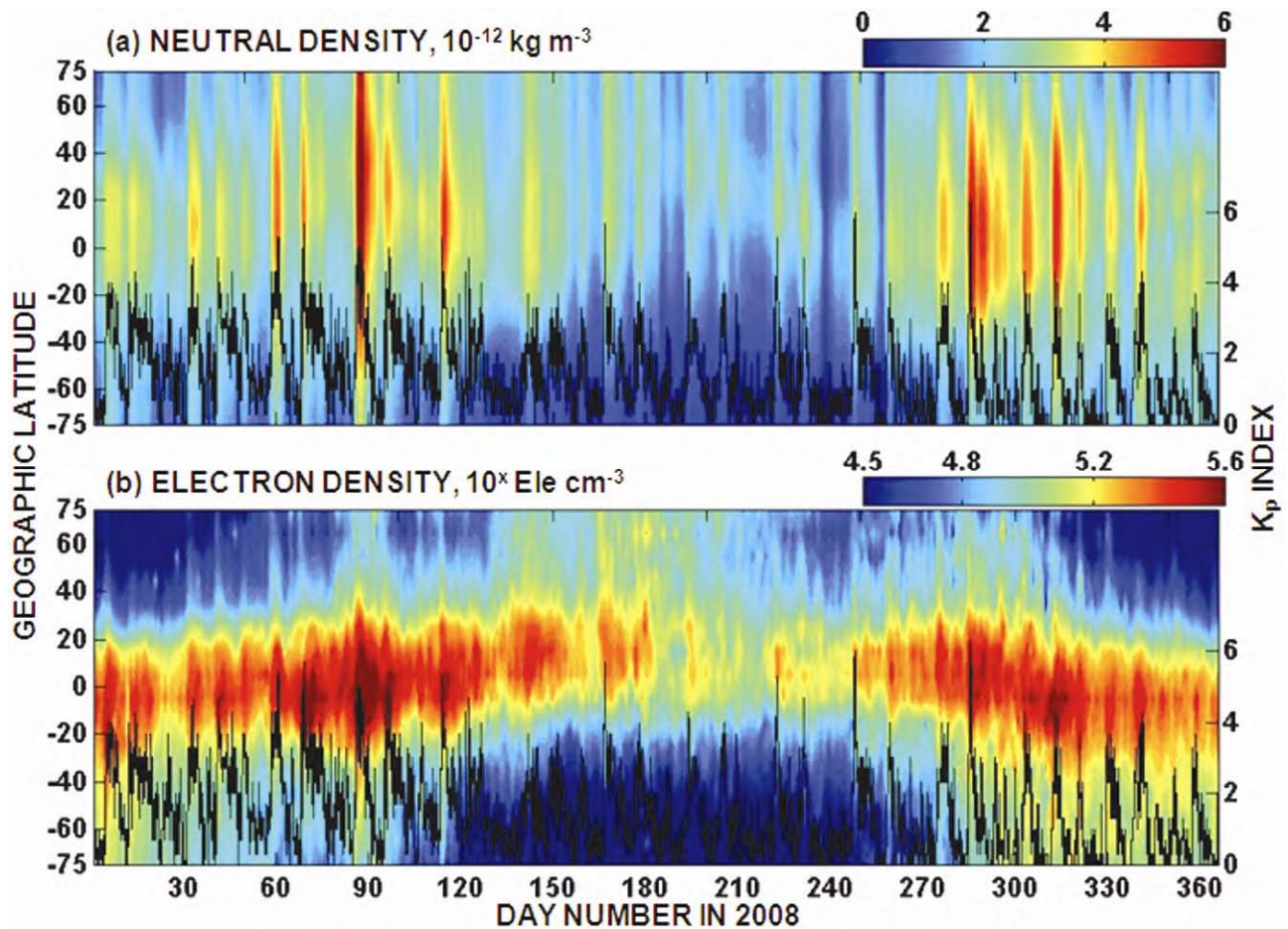


Fig. 4 — Variations of daily zonal mean: (a) neutral density from CHAMP; and (b) electron density from F3/C observations at 400 km altitude as a function of geographic latitude and day number in the year 2008; Overlapped black solid line indicates the variation of 3 h geomagnetic activity Kp index with scale on right hand side axis

quasi-periodic oscillations in Kp index are also superimposed in Figs 5(c and d) as black curve (right hand side scale). It can be observed from this figure that the perturbations in the zonal mean neutral density sometimes exceed 60% (peak-to-peak) with respect to background levels [Fig. 5(c)]. In comparison, the perturbations in electron density are smaller than those in neutral density. However, the perturbations in zonal electron density are larger in the respective winter hemispheres than in the summer hemispheres and can be as large as 60% of background values [Fig. 5(d)]. The higher percentage electron density perturbations in the winter hemispheres could be due to lower background electron densities in the respective winter hemispheres as can be observed from Fig. 4(b). For better visibility, the 9-day quasi periodic perturbations in both neutral density and electron density for a period of 60 days (± 30 days) centered on vernal

equinox are shown in Figs 6(a and b). It can be clearly seen from the Fig. 6 [as well as Figs 5(c and d)] that the quasi 9-day periodic enhancements in both neutral density and electron density at 400 km altitude are in phase with the enhancements in Kp. It should be mentioned that the F10.7 solar flux index and solar EUV irradiance do not exhibit any significant spectral peaks at 13.5 and 9-day periods [Figs 3(a and b)]. Therefore, from the results presented in Figs (4-6), the coherent enhancements in zonal mean neutral and electron densities at 400 km and good correlation in their spectral amplitudes with Kp index at sub-harmonic solar rotational periodicities can be attributed as due to recurrent geomagnetic activity associated with HSS-CIR structures.

4 Discussions

The SW-HSS contain high amplitude nonlinear Alfvén waves within the CIRs^{37,38}. The negative Bz

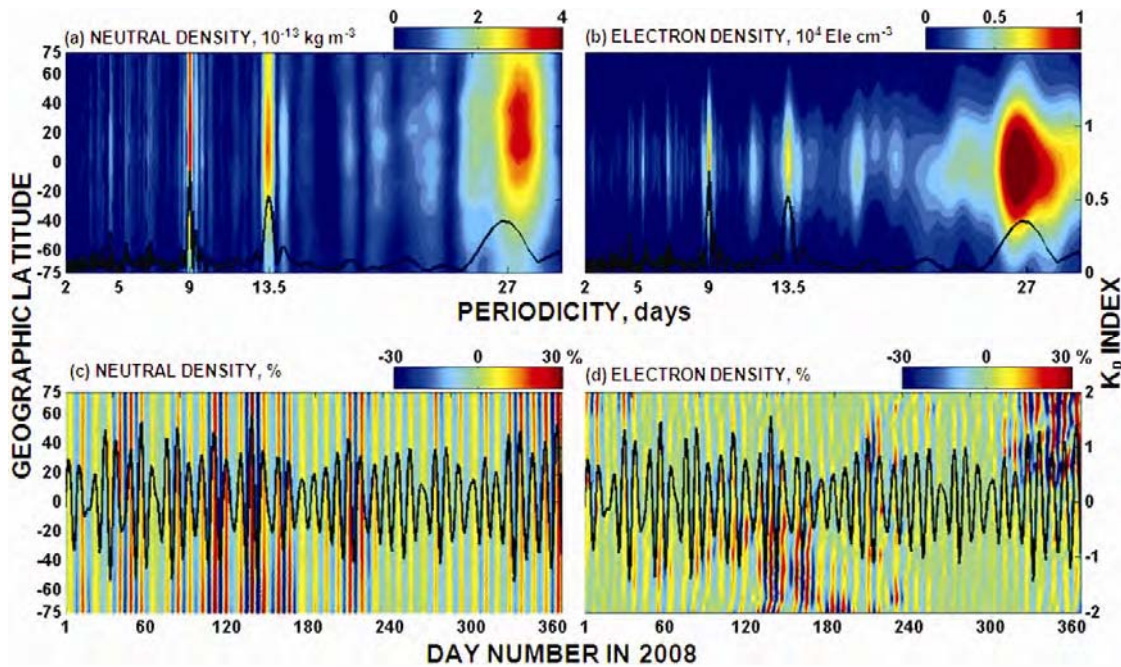


Fig. 5 — (a-b) Lomb-Scargle (LS) periodograms of: (a) neutral density, and (b) electron density, at 400 km altitude during the year 2008 (overlapped black curve indicates the LS periodogram of Kp index with right hand side scale); (c-d) band-pass filtered quasi 9-day periodic oscillations in: (c) neutral density, and (d) electron density (band-pass filtered quasi 9-day perturbations in Kp index also superimposed as a black solid curve with right hand side scale)

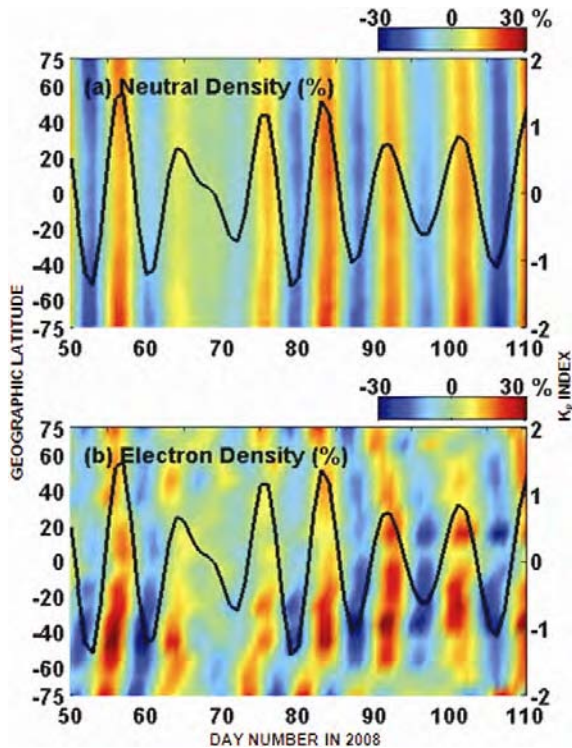


Fig. 6 — Expanded view of band-pass filtered quasi 9-day perturbations in: (a) neutral density, and (b) electron density for the period from day number 50 to 110 in 2008; superimposed black curve represents the band-pass filtered quasi 9-day perturbations in Kp index

components of the Alfvén waves within the HSS lead to magnetic reconnection and transfer of energy from the SW to the magnetosphere^{33,34}, which is characterized by continuous auroral activity called high intensity long duration continuous auroral activity (HILDCAA). The magnetic reconnection associated with Alfvén waves cause continuous, shallow injections of SW plasma into the magnetosphere at auroral and mid-latitudes. Further, it can be seen from the Figs (2 and 3) that the AE index and Kp index, which are the useful parameters for representing the particle precipitation at auroral and mid-latitudes^{39,40}, also exhibit concurrent enhancements with SW velocity. Therefore, it can be concluded that the fast SW streams from CHs, enhanced magnetic field and Alfvén-wave associated magnetic field fluctuations in HSS-CIR structures trigger recurrent geomagnetic activity of moderate to weak levels in the geospace environment at sub-harmonic solar rotational periodicities.

It is known that a series of changes takes place in the thermosphere and ionosphere during the geomagnetic storm periods. The high latitude thermosphere gets heated and thermally expands due to enhanced energy input that leads to an increase in the scale height of neutral as well as ionized upper atmosphere^{41,42}. Increased high latitude heating sets

up equatorward neutral winds, upwelling at the high latitudes and downwelling at low latitudes, which will significantly alter the thermospheric composition and hence, alter the ionospheric electron density⁴³⁻⁴⁶. In addition, equatorward neutral winds lift the plasma along the field lines into the altitude regions of reduced recombination rates^{43,44}. Further, the electric field perturbations due to prompt penetration electric fields (PPEF) and ionospheric disturbance dynamo (IDD) will alter the ionospheric electron density distribution in a complex manner that depends on the local time, geographic location, season as well as the phase of the geomagnetic storm⁴⁷⁻⁵⁴.

The coherent enhancements in neutral density and electron density concurrently with the enhancements in Kp index suggest the mechanism of thermal expansion. When the Joule and particle heating occur at high latitudes during the geomagnetic activity, the heated thermosphere expands and leads to an increase in the neutral scale height ($kT \text{ mg}^{-1}$). While this effect is larger at high latitudes, the atmospheric pressure tends to equilibrate globally, and the corresponding expansion occurs at all latitudes. It has been shown in earlier reports^{15,55} that the neutral density exhibits enhancements globally at all latitudes via thermal expansion during the recurrent CIR events. The plasma temperature changes associated with CIRs would also cause similar changes in the plasma scale height, which is a measure of thickness of the ionosphere. An increase in the scale height via thermal expansion associated with the plasma temperature will cause similar increase in F2 layer peak altitudes ($h_m F2$) and F2 layer thickness (H_T) (Ref. 16). Therefore, if one measures the electron density at any fixed height in the topside ionosphere (400 km), an increase or decrease in scale height causes a corresponding increase or decrease in electron density, respectively. Thus, the positive response in neutral density and electron density at 400 km shown in Fig. 4 is mainly related to corresponding changes in the neutral and plasma scale heights via thermal expansion associated with CIRs. Further, the equatorward wind during the enhanced geomagnetic activity will also raise the F layer to higher altitudes. This will also contribute to the concurrent enhancements in electron densities due to reduced recombination loss at higher altitudes. On the other hand, during the enhanced geomagnetic activity periods, the upwelling wind at high latitudes carries molecular-rich air to higher altitudes that will cause a decrease in the O/N_2 ratio, which in turn causes a

decrease in electron density. However, coherent enhancements in neutral density and electron density observed in Figs (4 and 5) suggest that thermal expansion is the dominant mechanism in the topside ionosphere (400 km) and the changes in neutral composition brought about by the thermospheric circulation is less effective at these altitudes.

Further, one would also expect that these moderate geomagnetic storms induced by recurrent HSS-CIRs structures may also cause electric field perturbations and thereby, alter the electron density distribution. In order to examine this, the H-component of geomagnetic field data from two magnetometers at Tirunelveli and Alibagh from the Indian region have been considered. The difference between the ΔH values (H-component of the magnetic field after subtracting the nighttime base level) at Tirunelveli and Alibagh, i.e., ΔH_{T-A} (nT) is taken as the strength of equatorial electrojet (EEJ)^{56,57}, which can be considered as a proxy to the zonal electric field at the equatorial latitudes⁵⁸⁻⁶⁰. For example, Fig. 7(a) shows the variation of EEJ strength (hourly values) during this low solar activity year 2008 and its LS periodogram is presented in Fig. 7(b). The horizontal dashed line in Fig. 7(b) represents the 95% significant level. It can be seen from this figure that EEJ strength exhibits significant day-to-day and seasonal variability with larger day time maxima around equinoxes and smaller values during the solstices⁶¹. The LS periodogram of EEJ strength shows strong spectral peaks 1-day, 0.5-day and 0.3-day corresponding to diurnal, semi-diurnal and ter-diurnal components of EEJ variation. However, the EEJ strength does not exhibit any significant spectral peaks at solar rotational (27-day) and its sub-harmonic periodicities (13.5 and 9-days). This suggests that the recurrent geomagnetic activity associated with HSS-CIR structures during this low solar activity year 2008 do not have significant impact on the EEJ strength. The perturbations in the zonal electric field during the geomagnetic storms are primarily due to prompt penetration and ionospheric disturbance dynamo processes, which generally depends on several factors like local time, southward/northward orientation of IMF Bz and its duration, intensity as well as the phase of the geomagnetic storm^{26,27,45-54}. Since the intensity of geomagnetic storms produced by HSS-CIR structures is small to moderate (~ -40 to -60 nT) and highly oscillatory nature of IMF Bz at the stream-stream interface

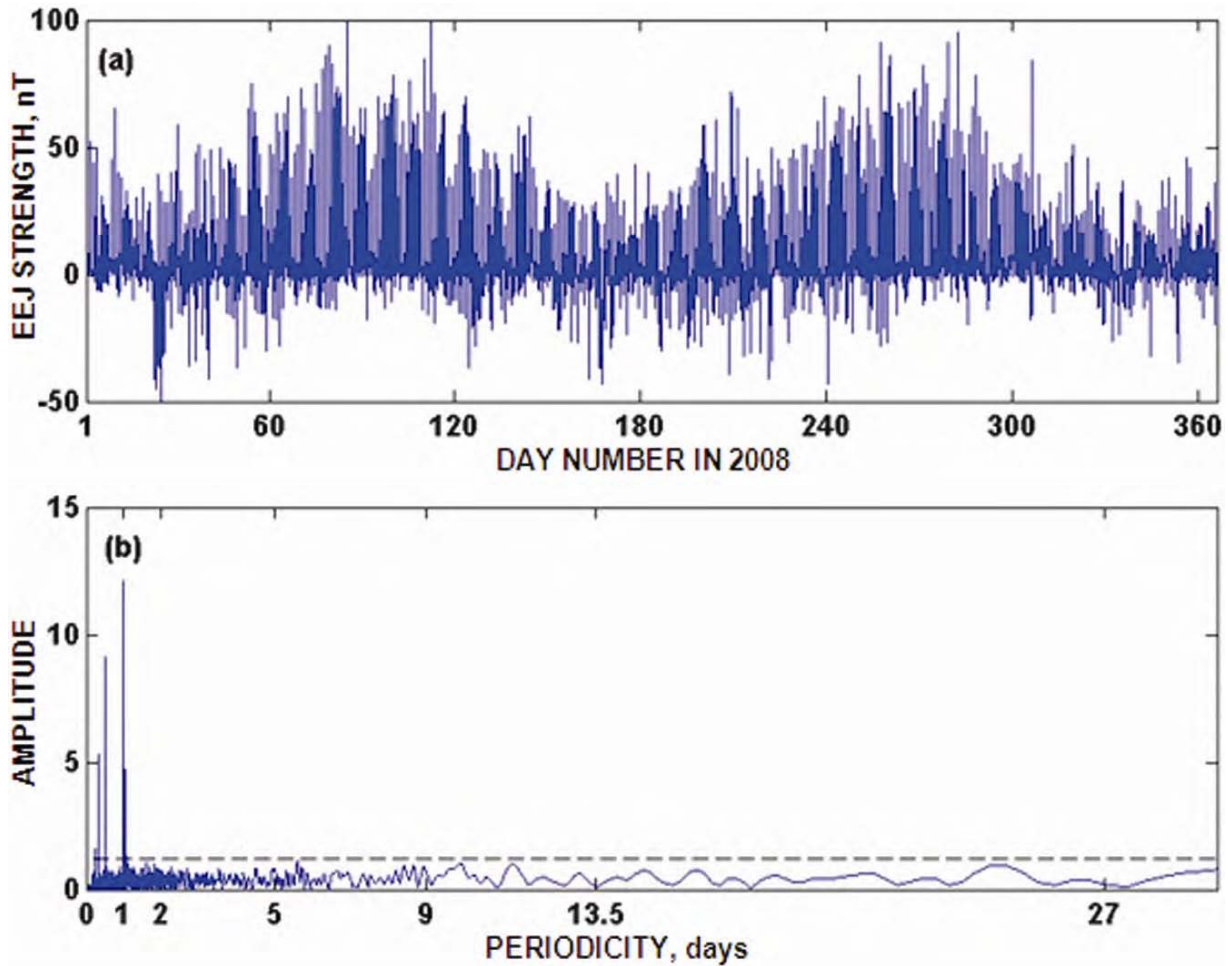


Fig. 7 — (a) Variations of the equatorial electrojet (EEJ) strength (hourly values) during extremely low solar activity year 2008; and (b) the corresponding LS periodogram

region, it may not be possible to produce significant perturbations in zonal electric field via prompt penetration. Also, the local time at the onset of each CIR induced storm is not same at the location of EEJ observations (Indian sector). Hence, the perturbations in the zonal electric field, even if induced, were not uniform for each CIR-storm. Similar argument also applies for electric field perturbations induced by ionospheric disturbance dynamo process. Hence, one cannot see any recurrent signatures in EEJ strength corresponding to those periodicities in recurrent CIR-induced geomagnetic activity. Instead, one needs to study carefully case-by-case for each CIR storm in order to assess the role of CIR induced geomagnetic activity on zonal electric field perturbations.

5 Summary

The extreme low solar activity year 2008 is unique with more than 70% spotless days and F10.7 solar

flux is steadily at low values of ~ 70 sfu for a prolonged period. However, the geospace environment is not so quiet and significantly perturbed by recurrent solar and magnetospheric driven disturbances. A detailed analysis of solar wind and magnetic properties reveal that the solar wind high speed streams from the low latitude coronal holes during this low solar activity period were the primary contributor for a series of corotating interaction regions (CIRs) in the interplanetary medium. The resultant HSS - CIR structures of enhanced density and magnetic field regions recurrently impinge on the Earth's magnetosphere. The magnetic reconnection associated with Alfvén waves in the HSS - CIR structures cause continuous, shallow injections of SW plasma into the magnetosphere and trigger recurrent geomagnetic activity of weak to moderate levels in the geospace environment (Fig. 1). Further, the LS amplitude spectra (Fig. 3) of the SW parameters, and

geomagnetic activity indexes (AE, Kp and SymH) show similar features, with strong spectral peaks at sub-harmonic solar rotational periodicities (13.5 and 9-day periods). Results shown in Figs (2 and 3) clearly suggest that these periodicities in geomagnetic activity are primarily due to SW energy input associated with CIR structures within fast SW streams from recurrent CHs.

The response of thermosphere and ionosphere system to this recurrent geomagnetic activity is investigated using the neutral density and electron density measurements at an altitude of 400 km by CHAMP and F3/C satellites (Fig. 4). The LS spectra of both the neutral density and electron density exhibit predominant spectral amplitudes at solar rotational (27-day) and its sub-harmonic (13.5 and 9-day) periodicities which further correlate well with spectral amplitudes in Kp index [Figs 5(a and b)]. The important feature of 9-day periodicity is considered to examine the phase relationship between the perturbations in neutral density and electron density with the recurrent geomagnetic activity. Both the neutral density and electron density exhibit coherent enhancements concurrently with the Kp. This suggests that the thermospheric and ionospheric response at 400 km (topside ionosphere) is generally dominated by changes in temperature and increase in scale height via thermal expansion due to recurrent geomagnetic activity associated with HSS-CIR structures. The strength of equatorial electrojet (EEJ) derived from ground based magnetometers does not show any significant spectral amplitude at sub-harmonic solar rotational periodicities. This suggests that weak to moderate level of recurrent geomagnetic storms produced by HSS-CIR structures does not show significant impact in the equatorial zonal electric field during this low solar activity year 2008. Nevertheless, a further investigation is needed on a case-by-case basis to understand the impact of CIR-storms on equatorial zonal electric field and its implications.

Acknowledgements

The work of one of authors, STR, is partly supported by Japan Society for Promotion of Science (JSPS) Foundation. The authors sincerely thank the Director, Indian Institute of Geomagnetism (IIG), India for providing the magnetometer data through their website (<http://www.wdciig.res.in/select1.asp>). The authors also greatly acknowledge the open

data policy of the UCAR/CDAC, NSPO for Formosat-3/COSMIC data, CHAMP-GRACE team in University of Colorado for CHAMP accelerometer data, ACE Science Center and NSSDC for solar wind and magnetic data, the WDC for geomagnetic data and the TIMED - SEE team for EUV irradiance data.

References

- 1 Sagawa E, Immel T J, Frey H U & Mende S B, Longitudinal structure of the equatorial anomaly in the nighttime ionosphere observed by IMAGE/FUV, *J Geophys Res (USA)*, 110 (2005) A11302, doi: 10.1029/2004JA010848.
- 2 Immel T J, Sagawa E, England S L, Henderson S B, Hagan M E, Mende S B, Frey H U, Swenson C M & Paxton L J, Control of equatorial ionospheric morphology by atmospheric tides, *Geophys Res Lett (USA)*, 33 (2006) L15108, doi: 10.1029/2006GL026161.
- 3 Lin C H, Hsiao C C, Liu J Y & Liu C H, Longitudinal structure of the equatorial ionosphere: Time evolution of the four-peaked EIA structure, *J Geophys Res (USA)*, 112 (2007) A12305, doi: 10.1029/2007JA012455.
- 4 Tulasi Ram S, Su S -Y & Liu C H, FORMOSAT-3/COSMIC observations of seasonal and longitudinal variations of equatorial ionization anomaly and its inter-hemispheric asymmetry during the solar minimum period, *J Geophys Res (USA)*, 114 (2009) A06311, doi: 10.1029/2008JA013880.
- 5 Goncharenko L & Zhang S, Ionospheric signatures of sudden stratospheric warming: Ion temperature at middle latitude, *Geophys Res Lett (USA)*, 35 (2008) L21103, doi: 10.1029/2008GL035684.
- 6 Chau J L, Fejer B G & Goncharenko L P, Quiet variability of equatorial $E \times B$ drifts during a sudden stratospheric warming event, *Geophys Res Lett (USA)*, 36 (2009) L05101, doi: 10.1029/2008GL036785.
- 7 Goncharenko L P, Chau J L, Liu H & Coster A J, Unexpected connections between the stratosphere and ionosphere, *Geophys Res Lett (USA)*, 37 (2010a) L10101, doi: 10.1029/2010GL043125.
- 8 Goncharenko L P, Coster A J, Chau J L & Valladares C E, Impact of sudden stratospheric warmings on equatorial ionization anomaly, *J Geophys Res (USA)*, 115 (2010b) A00G07, doi: 10.1029/2010JA015400.
- 9 Fejer B G, Olson M E, Chau J L, Stolle C, Lühr H, Goncharenko L P, Yumoto K & Nagatsuma T, Lunar-dependent equatorial ionospheric electrodynamic effects during sudden stratospheric warmings, *J Geophys Res (USA)*, 115 (2010) A00G03, doi: 10.1029/2010JA015273.
- 10 Liu H, Doornbos E, Yamamoto M & Tulasi Ram S, Strong thermospheric cooling during the 2009 major stratosphere warming, *Geophys Res Lett (USA)*, 38 (2011) L12102, doi: 10.1029/2011GL047898.
- 11 Pancheva D V et al., Two-day wave coupling of the low-latitude atmosphere-ionosphere system, *J Geophys Res (USA)*, 111 (2006) A07313, doi: 10.1029/2005JA011562.
- 12 Abdu M, Ramkumar T K, Batista I S, Brum C G, Takahashi H, Reinisch B W & Sobra I H, Planetary wave signatures in the equatorial atmosphere-ionosphere system and mesosphere, E- and F-region coupling, *J Atmos Sol-Terr Phys (UK)*, 68 (2006) pp 509–522.

- 13 Lastovicka J, Forcing of the ionosphere by waves from below, *J Atmos Sol-Terr Phys (UK)*, 68 (2006) pp 479–497.
- 14 Sathishkumar S & Sridharan S, Observations of 2–4 day inertia-gravity waves from the equatorial troposphere to the F region during the sudden stratospheric warming event of 2009, *J Geophys Res (USA)*, 116 (2011) A12320, doi: 10.1029/2011JA017096.
- 15 Lei J, Thayer J P, Forbes J M, Sutton E K & Nerem R S, Rotating solar CHs and periodic modulation of the upper atmosphere, *Geophys Res Lett (USA)*, 35 (2008a) L10109, doi: 10.1029/2008GL033875.
- 16 Tulasi Ram S, Lei J, Su S -Y, Liu C H, Lin C H & Chen W S, Dayside ionospheric response to recurrent geomagnetic activity during the extreme solar minimum of 2008, *Geophys Res Lett (USA)*, 37 (2010) L02101, doi: 10.1029/2009GL041038.
- 17 Phillips J L *et al.*, Ulysses solar wind plasma observations at high southerly latitudes, *Science (USA)*, 268 (5213) (1995) pp 1030–1033.
- 18 Krieger A S, Timothy A F & Roelof E C, A CH and its identification as the source of a high velocity solar wind stream, *Sol Phys (Netherlands)*, 29 (1973) pp 505–525.
- 19 Sheeley N R Jr & Harvey J W, Coronal holes, solar wind streams, and recurrent geomagnetic disturbances during 1978 and 1979, *Sol Phys (Netherlands)*, 70 (1981) pp 237–249.
- 20 Tsurutani B T, Gonzalez W D, Gonzalez A L C, Tang F, Arballo J K & Okada M, Interplanetary origin of geomagnetic activity in the declining phase of the solar cycle, *J Geophys Res (USA)*, 100 (A11) (1995) pp 21, 717–21,733.
- 21 Prohls G W, Magnetic storm associated perturbation of the upper atmosphere: Recent results obtained by satellite-borne gas analyzers, *Rev Geophys (USA)*, 18 (1980) pp 183–202.
- 22 Fuller-Rowell T J, Coderscu M V, Rishbeth H, Moffett R J & Quegan S, On the seasonal response of the thermosphere and ionosphere to geomagnetic storms, *J Geophys Res (USA)*, 101 (1996) pp 2343–2353.
- 23 Fuller-Rowell T J, Codrescu M V, Moffett R J & Quegan S, Response of the thermosphere and ionosphere to geomagnetic storms, *J Geophys Res (USA)*, 99 (1994) pp 3893–3914.
- 24 Buonsanto M J, Ionospheric Storms - A Review, *Space Sci Rev (Netherlands)*, 88 (1999) pp 563–601.
- 25 Mendillo M, Storms in the ionosphere: Patterns and processes for total electron content, *Rev Geophys (USA)*, 44 (2006) RG4001, doi: 10.1029/2005RG000193.
- 26 Sastri J H, Equatorial electric fields of ionospheric disturbance dynamo origin. *Ann Geophys (France)*, 6 (1988) pp 635–642.
- 27 Sastri J H, Niranjan K & Subbarao K S V, Response of the equatorial ionosphere in the Indian (midnight) sector to the severe magnetic storm of July 15, 2000, *Geophys Res Lett (USA)*, 29 (13) (2002) pp 1651–1655, doi: 10.1029/2002GL015133.
- 28 Mendillo M & Schatten K, Influence of solar sector boundaries on ionospheric variability, *J Geophys Res (USA)*, 88(A11) (1983) pp 9145–9153.
- 29 Richardson I G, Energetic particles and corotating interaction region in the solar wind, *Space Sci Rev (Netherlands)*, 111 (2004) pp 267–376.
- 30 Lee C O, Luhmann J G, Zhao X P, Liu Y, Riey P, Arge C N, Russell C T & de Pater I, Effects of the weak polar fields of solar cycle 23: Investigation using OMNI for the STEREO mission period, *Sol Phys (Netherlands)*, 256 (2009) pp 345–363, doi: 10.1007/s11207-009-9345-6.
- 31 Kennel C F, Arons J, Blandford R, Coroniti F, Israel M, Lanzerotti L, Lightman A, Papadopoulos K, Rosner R & Scarf F, Perspectives on space and astrophysical plasma physics, unstable current systems and plasma instabilities in astrophysics, in *Unstable Current Systems and Plasma Instabilities in Astrophysics; Proceedings of the 107th Symposium*, edited by M R Kundu & G D Holman (D Reidel, Dordrecht), 1985, pp 537–552.
- 32 Tsurutani B T, Echer E, Guarnieri F L & Kozyra J U, CAWSES November 7–8, 2004, superstorm: Complex solar and interplanetary features in the post-solar maximum phase, *Geophys Res Lett (USA)*, 35 (2008) L06S05, doi: 10.1029/2007GL031473.
- 33 Tsurutani B T & Gonzalez W D, The cause of high intensity long-duration continuous AE activity (HILDCAAs): Interplanetary Alfvén wave trains, *Planet Space Sci (UK)*, 35 (1987) 405.
- 34 Tsurutani B T *et al.*, Corotating solar wind streams and recurrent geomagnetic activity: A review, *J Geophys Res (USA)*, 111 (2006), A07S01, doi: 10.1029/2005JA011273.
- 35 Lomb N R, Least-squares frequency analysis of unequally spaced data, *Astrophys Space Sci (Netherlands)*, 39 (1976) pp 447–462.
- 36 Scargle J D, Studies in astronomical time series analysis. II. Statistical aspects of spectral analysis of unevenly spaced data, *Astrophys J (USA)*, 263 (1982) pp 835–853.
- 37 Tsurutani B T, Ho C M, Smith E J, Neugebauer M, Goldstein B E, Mok J S, Arballo J K, Balogh A, Southwood D J & Feldman W C, The relationship between interplanetary discontinuities and Alfvén waves: Ulysses observations, *Geophys Res Lett (USA)*, 21 (1994), 2267.
- 38 Balogh A, Smith E J, Tsurutani B T, Southwood D J, Forsyth R J & Horbury T S, The heliospheric magnetic field over the south polar region of the sun, *Science (USA)*, 268 (5218) (1995) pp 1007–1010.
- 39 Emery B A, Coumans V, Evans D S, Germany G A, Greer M S, Holeman E, Kadinsky-Cade K, Rich F J & Xu W, Seasonal, Kp, solar wind, and solar flux variations in long-term single-pass satellite estimates of electron and ion auroral hemispheric power, *J Geophys Res (USA)*, 113 (2008), A06311, doi: 10.1029/2007JA012866.
- 40 Emery B A, Richardson I G, Evans D S & Rich F J, Solar wind structure sources and periodicities of auroral electron power over three solar cycles, *J Atmos Sol-Terr Phys (UK)*, 71 (2009) pp 1157–1175.
- 41 Prohls G W, Magnetic storm associated perturbation of the upper atmosphere: Recent results obtained by satellite-borne gas analyzers, *Rev Geophys (USA)*, 18 (1980) pp 183–202.
- 42 Roble R G, Dickinson R E & Ridley E C, Global circulation and temperature structures of thermosphere with high-latitude convection, *J Geophys Res (USA)*, 87 (1982) 1599.

- 43 Fuller-Rowell T J, Codrescu M V, Moffett R J & Quegan S, Response of the thermosphere and ionosphere to geomagnetic storms, *J Geophys Res (USA)*, 99 (1994) pp 3893–3914.
- 44 Fuller-Rowell T J, Codrescu M V, Rishbeth H, Moffett R J & Quegan S, On the seasonal response of the thermosphere and ionosphere to geomagnetic storms, *J Geophys Res (USA)*, 101 (1996) pp 2343–2353.
- 45 Chandra S & Herman J R, F-region ionization and heating during magnetic storms, *Planet Space Sci (UK)*, 17 (1969) pp 841–851.
- 46 Sastri J H & Titheridge J E, Depressions in midlatitude F-region under relatively quiet geomagnetic conditions, *J Atmos Sol-Terr Phys (UK)*, 39 (1977) pp 1307–1316.
- 47 Rastogi R G, Geomagnetic storms and electric fields in the equatorial ionosphere, *Nature (UK)*, 268 (1977) 422.
- 48 Spiro R W, Wolf R A & Fejer, Penetration of high latitude electric field effects to low latitudes during SUNDIAL 1984, *Ann Geophys (France)*, 6 (1) (1988) pp 39–50.
- 49 Blanc M & Richmond A D, The ionospheric disturbance dynamo, *J Geophys Res (USA)*, 85 (1980) pp 1669–1688.
- 50 Mendillo M, Storms in the ionosphere: Patterns and processes for total electron content, *Rev Geophys (USA)*, 44 (2006) RG4001, doi: 10.1029/2005RG000193.
- 51 Tulasi Ram S, Rama Rao P V S, Prasad D S V V D, Niranjan K, Gopi Krishna S, Sridharan R & Ravindran S, Local time dependent response of postsunset ESF during geomagnetic storms, *J Geophys Res (USA)*, 113 (2008) A07310, doi: 10.1029/2007JA012922.
- 52 Basu S, Basu Su, Rich F J, Groves K M, MacKenzie E, Coker C, Sahai Y, Fagundes P R & Becker-Guedes F, Response of the equatorial ionosphere at dusk to penetration electric fields during intense geomagnetic storms, *J Geophys Res (USA)*, 112 (2007) A08308, doi: 10.1029/2006JA012192.
- 53 Vijaya Lekshmi D, Balan N, Tulasi Ram S & Liu J Y, Statistics of geomagnetic storms and ionospheric storms at low and mid latitudes in two solar cycles, *J Geophys Res (USA)*, 116 (2011) A11328, doi: 10.1029/2011JA017042.
- 54 Balan N & Rao P B, Dependence of ionospheric response on the local time of sudden commencement and intensity of storms, *J Atmos Terr Phys (UK)*, 52 (1990) pp 269–275.
- 55 Thayer J P, Lei J, Forbes J M, Sutton E K & Nerem R S, Thermospheric density oscillations due to periodic solar wind high-speed streams, *J Geophys Res (USA)*, 113 (2008) A06307, doi: 10.1029/2008JA013190.
- 56 Rusch C M & Richmond A D, The relationship between the structure of the equatorial anomaly and the strength of the equatorial electrojet, *J Atmos Sol-Terr Phys (UK)*, 35 (1973) pp 1171–1180.
- 57 Rastogi R G & Klobuchar J A, Ionospheric electron content within the equatorial F2 layer anomaly belt, *J Geophys Res (USA)*, 95 (1990) 19,045–19,052.
- 58 Anderson D, Anghel A, Yumoto K, Ishitsuka M & Kudeki E, Estimating daytime vertical E_B drift velocities in the equatorial F-region using ground-based magnetometer observations, *Geophys Res Lett (USA)*, 29(12) (2002) 1596, doi: 10.1029/2001GL014562.
- 59 Rastogi R G, Geomagnetic field variations at low latitudes and ionospheric electric field, *J Atmos Terr Phys (UK)*, 55 (1993) pp 1375–1381.
- 60 Chandra H, Misra R K & Rastogi R G, Equatorial ionospheric drift and the electrojet, *Planet Space Sci (UK)*, 19 (1971) pp 1497–1503.
- 61 Rastogi R G, Alex S & Patil A, Seasonal variation of geomagnetic D, H and Z fields at low latitudes, *J Geomagn Geoelectr (Japan)*, 46 (1994) pp 115–126.